ISSN 1063-7826, Semiconductors, 2015, Vol. 49, No. 8, pp. 1012–1018. © Pleiades Publishing, Ltd., 2015.
Original Russian Text © V.M. Kalygina, Yu.S. Petrova, I.A. Prudaev, O.P. Tolbanov, S.Yu. Tsupiy, 2015, published in Fizika i Tekhnika Poluprovodnikov, 2015, Vol. 49, No. 8, pp. 1036–1042.

SEMICONDUCTOR STRUCTURES, LOW-DIMENSIONAL SYSTEMS, AND QUANTUM PHENOMENA

Deep Centers in TiO_2–Si Structures

V. M. Kalygina*, Yu. S. Petrova, I. A. Prudaev, O. P. Tolbanov, and S. Yu. Tsupiy

National Research Tomsk State University, Tomsk, 634050 Russia

**e-mail: Kalygina@ngs.ru*

Submitted November 11, 2014; accepted for publication December 22, 2014

Abstract—The effects of thermal annealing and exposure to oxygen plasma on the electrical and photoelectric properties of metal–TiO_2–Si structures are investigated. The TiO_2 films are fabricated by the rf magnetron sputtering of a titanium-oxide target onto unheated *n*-Si substrates. The forward and reverse currents of the structures after annealing in argon at 500°C are lower than those after annealing at 750°C. Exposure of the titanium-dioxide films to oxygen plasma led to a decrease in the currents at all annealing temperatures. It is supposed that the *I–V* characteristics of the TiO_2–Si structures can be described using the model of space-charge-limited currents. The photoelectric characteristics of the samples are investigated via illumination at a wavelength of $\lambda = 400$ nm. The TiO_2–Si structures annealed at 500°C without exposure to oxygen plasma exhibit frozen photoconductivity. The relaxation time is 23 ± 2 min.

DOI: 10.1134/S1063782615080102

1. INTRODUCTION

Defects in TiO_2 are an important factor that determines the physical and chemical properties of titanium oxide. At present, there is a lack of agreement concerning the nature and specific role of point defects in titanium dioxide. Oxygen vacancies are believed to play the role of donor centers with shallow energy levels near the bottom of the conduction band. On the other hand, oxygen vacancies that captured one or two electrons transform into spin configurations with magnetic moments at Ti^{3+} [1]. The Ti^{3+} cations formed due to the transition of electrons from the lattice Ti^{4+} ions create deep traps for electrons with long lifetimes [2]. Xiong et al [3] described two main mechanisms of the formation of Ti^{3+} centers: the interband generation of electron–hole pairs under high-energy irradiation (UV radiation, electron flux, γ radiation, etc.) and the formation of Ti^{3+} cations on account of oxygen vacancies. It was demonstrated that the Ti^{3+} concentration increases with the number of oxygen vacancies upon the annealing of titanium-oxide powder in hydrogen.

Photoinduced Ti^{3+} centers are chemically active and have a long lifetime [4]. They play an important role in photocatalytic processes [5] and determine the hydrophilic properties of titanium-oxide films [6–8], photochromic effects [9], and features of the absorption spectra after high-energy irradiation [10]. A variety of widely applied phenomena with the involvement of trapping centers requires an understanding of their role in different processes, including the conductivity mechanism.

The behavior of electrons in the conduction band of TiO_2 and other metal-oxide materials determines their potential for application. Analysis of the available experimental data reveals contradictory facts. Optical and spin resonance investigations show the existence of small-radius polarons, whereas measurements of the electrical characteristics suggest rather a high mobility of carriers, which can be related only to the existence of delocalized free electrons [11].

The accumulation of experimental results on the properties of TiO_2 films is considered to be rather interesting and useful, in view of the ambiguity of available data on the nature of defects in titanium dioxide. Here, we report the results of investigations of the electrical characteristics of TiO_2–*n*-Si structures without illumination ("dark" characteristics) and under illumination at a wavelength of $\lambda = 400$ nm.

2. EXPERIMENTAL

90–100-nm-thick TiO_2 films were formed by rf magnetron sputtering on epitaxial silicon layers with a donor concentration of $N_d = 1.5 \times 10^{15}$ cm^{-3}. Then, the silicon substrate with the TiO_2 film was cut into two parts. Half of it was annealed in argon at 500°C (the first series) and the other half, at 750°C (the second series) for 30 min. Some samples from each series were exposed to oxygen plasma for 20 min at 50°C.

To measure the electrical characteristics, Ni/V electrodes were deposited by electron-beam evaporation onto the TiO_2 surface and rear side of the silicon substrate of the samples from both series. The electrode on the silicon surface was continuous and the electrodes on the titanium-dioxide surface were formed through masks. The diameter of the electrode

V characteristics

Series, temperature of annealing in argon	Oxygen-plasma treatment	Forward current I_{for}, A	Reverse current I_{rev}, A	Rectification factor K at $U = \pm 1$ V
First, 500°C	Without treatment, 20 min	3.03×10^{-5}	1.22×10^{-5}	2.49
		4.81×10^{-5}	2.71×10^{-9}	1.77×10^{4}
Second, 750°C	Without treatment, 20 min	2.72×10^{-4}	4.66×10^{-7}	5.84×10^{2}
		7.35×10^{-5}	1.27×10^{-8}	5.79×10^{3}

to TiO_2 (gate) was 1.15 mm and its area was $S = 1.04 \times 10^{-2}$ cm^2.

After the completion of all planned treatments, the silicon substrates were cut into individual chips. The technique for sample preparation and X-ray diffraction (XRD) and atomic force microscopy (AFM) data for the obtained titanium-dioxide films are described in more detail in [12].

The "dark" *I–V* characteristics and those under illumination at $\lambda = 520$ nm were measured using an automated setup for measuring currents in the range 10^{-9}–10^{-2} A at voltages in the range of ±30 V. The photoelectric characteristics were studied using a light-emitting diode (LED) with an emission wavelength of $\lambda = 400$ nm. The side of the TiO_2 film of the structures was illuminated. The emission power *P* was changed by varying the LED current.

3. RESULTS

Depending on the conditions of treatment of the Ni/V–Si–TiO_2–V/Ni (metal–insulator–semiconductor, MIS) structure, its *I–V* characteristics have different degrees of symmetry with respect to the polarity of the potential of the control electrode. Positive potential *U* at the gate corresponds to forward currents; the reverse currents are detected at negative potentials.

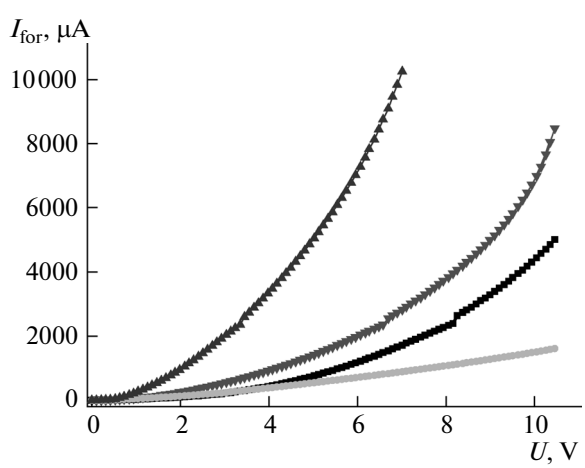

Fig. 1. Effect of oxygen plasma on the forward *I–V* characteristics of the Ni/V–Si–TiO_2–V/Ni structures after annealing in argon at (*1*, *2*) 500°C and (*1'*, *2'*) 750°C (*1*, *1'*) without pretreatment and (*2*, *2'*) after oxygen-plasma treatment.

The forward I_{for} and reverse I_{rev} currents at the voltages $U = \pm 1$ V for the structures annealed at 500 and 750°C without oxygen-plasma treatment and exposed to plasma for 20 min are given in the table. The rectification factor *K* is found to be the smallest after annealing in argon at 500°C and without exposure to plasma.

The metal–insulator–semiconductor structures with an amorphous-crystalline film annealed at 500°C without exposure to oxygen plasma exhibit lower forward currents as compared with the samples with the TiO_2 film annealed at 750°C [2]. These structures are characterized by a slight dependence of the "dark" currents on the sign of the gate potential in the voltage range $0 \le |U| \le 4$ V (see the table).

The *I–V* characteristics symmetric with respect to the gate potential in the voltage range *2* V were observed for the Al–TiO_2–*p*-Si and Pd–TiO_2–*n*-Si structures [13–15].

Annealing of the titanium-oxide films in argon at 750°C leads to an increase in the forward currents, while, after exposure to the oxygen plasma, the currents decrease independent of the annealing temperature (Fig. 1).

The reverse *I–V* characteristics are the most strongly affected by the oxygen plasma. For comparison, Fig. 2 shows the reverse *I–V* characteristics for several samples in argon at 500°C without and with preliminary exposure to oxygen plasma (Figs. 2a and 2b, respectively).

The data shown in Fig. 2 and given in the table demonstrate that oxygen-plasma treatment leads to a sharp drop in the reverse currents in the samples annealed at 500°C, while the forward current in the range $U \le 5$ V changes insignificantly. As a result, factor *K* for these samples sharply grows (see the table).

The structures annealed at 750°C are affected to a significantly less extent by the oxygen plasma. Both forward and reverse currents decrease by an order of magnitude and the rectification factor increases by a factor of ~10 (see the table).

The effect of light with $\lambda = 400$ nm (the photon energy is $h\nu = 3.1$ eV) barely changes the forward currents of the metal–TiO_2–*n*-Si structures in the case of

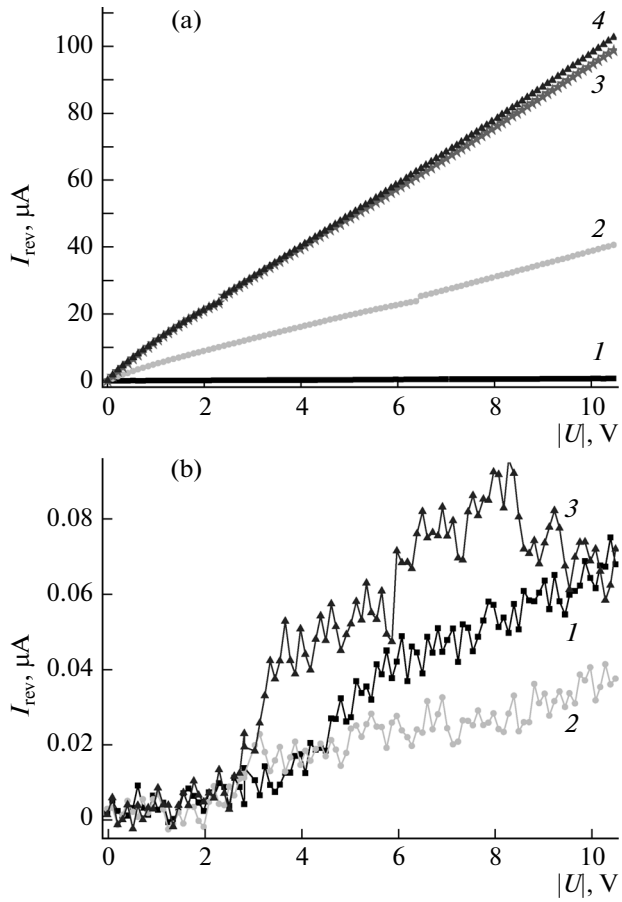

Fig. 2. Reverse currents for structures *1–4* (a) not exposed and (b) exposed to the oxygen plasma before annealing in argon at 500°C.

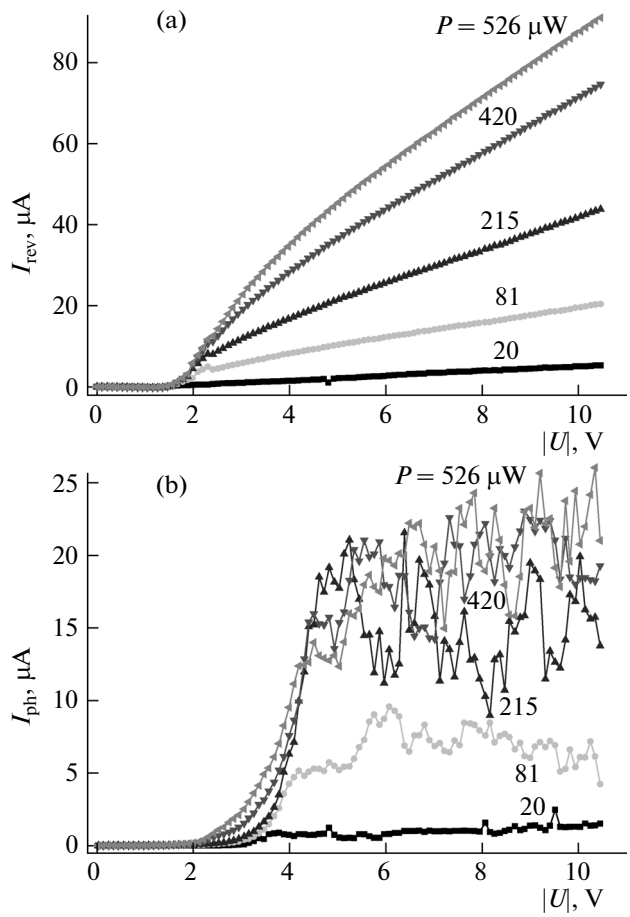

Fig. 3. Voltage dependence of the photocurrent for the samples (a) not exposed and (b) exposed to oxygen plasma and then annealed in argon at 500°C.

all treatments described here; the photocurrent is not observed at positive gate potentials and the *I–V* characteristics under illumination barely differ from the corresponding "dark" ones.

Under illumination at $\lambda = 400$ nm at negative gate potentials, photocurrent is detected in the structures and its value is determined by the optical power, voltage, and treatment conditions.

The photocurrent I_{ph} in the structures annealed at 500°C without preliminary exposure to oxygen plasma is independent of the optical power and voltage in the range $0 \le |U| \le 2$ V and has extremely small values at these voltages. In the coordinates $I_{ph}(U)$, the photocurrent increases starting from $|U| = 2$ V in accordance with sublinear law (Fig. 3a).

In the structures treated in the oxygen plasma, the dependence $I_{ph}(|U|)$ at low voltages $|U| \le 2$ V remains unchanged; as the voltage is increased, the photocurrent sharply increases starting from $|U| = 3–4$ V and tends to saturation at $|U| \ge 5$ V. With an increase in the optical power, the photocurrent grows (Fig. 3b), but the I_{ph} values for these samples are smaller than for the structures not treated in oxygen plasma.

The effect of light with $\lambda = 400$ nm on the Ni/V–Si–TiO_2–V/Ni structures annealed at 500°C with preliminary exposure to plasma for 20 min is characterized by a slow decrease in the reverse currents after the end of exposure. In Figure 4, the numbers near the curves indicate the time after switching off the illumination with $P = 520$ μW(I_L is the current at $P = 520$ μW and I_d is the initial "dark" current before illumination). Even after 3 h, the "dark" *I–V* characteristic does not return to the initial curve (lower curve in Fig. 4) and the reverse "dark" current after illumination at $\lambda = 400$ nm remains higher than the initial value. Figure 5 shows the dependences of the reverse current on the time after switching off the light for several reverse voltages on the sample. The form of the curves is independent of $|U|$.

After annealing at 750°C, the voltage at which the photocurrent starts growing sharply with increasing $|U|$ lowers by a factor of almost two and its values increase as compared with the samples annealed at 500°C (Figs. 6a and 6b). Thus, independent of the annealing temperature, there exists a threshold voltage U_t starting at which the photocurrent appears in the

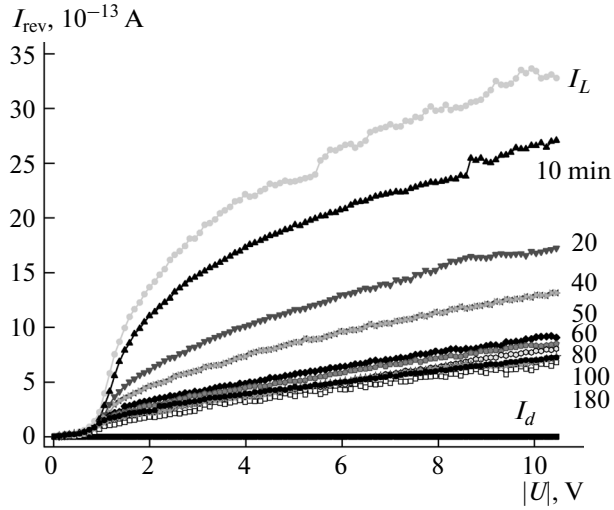

Fig. 4. Voltage dependences of the reverse "dark" current at different times for the sample annealed in argon at 500°C and exposed to oxygen plasma before annealing. I_L is the current under illumination and I_d is the "dark" current.

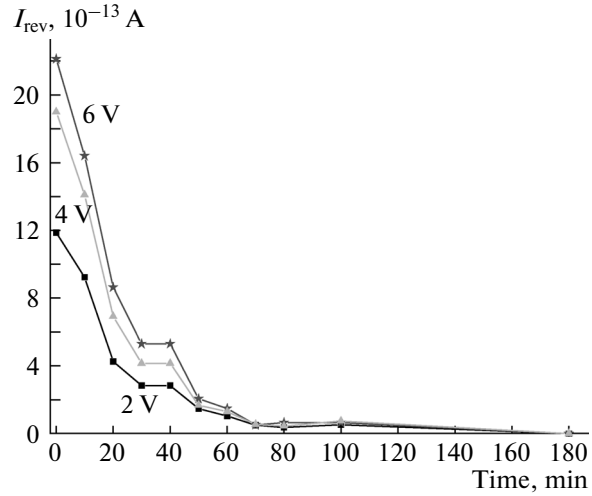

Fig. 5. Time dependence of the "dark" current at a fixed voltage after switching off the light (the voltage values are indicated).

Ni/V–Si–TiO_2–V/Ni structures at negative gate voltages. For the samples with the TiO_2 film in the rutile phase, the U_t values are half as large as for the structures with TiO_2 in the anatase phase.

After switching off the light, the reverse current decreases instantaneously, but, for the structures not treated in oxygen plasma after annealing in argon at 750°C, the reverse currents appear two times smaller than the initial ones before illumination at $\lambda = 400$ nm (Fig. 7a). This effect is observed for all of the investigated samples and can be used to lower the leakage currents in metal–Si–TiO_2–metal structures.

Pretreatment with oxygen plasma did not change the dependence $I_{ph}(|U|)$ for the samples annealed at 750°C, but, as for samples from the first series, the photocurrent was smaller than for the samples not exposed to plasma (Fig. 6). After switching off the illumination, the reverse "dark" current was larger than its initial value or returned to the initial values (Fig. 7b).

4. DISCUSSION

The specific features in the behavior of the electrical and photoelectric properties of the investigated samples are determined by the structure and phase composition of the TiO_2 film on the surface of a silicon substrate [2].

The effect of oxygen plasma on the TiO_2–Si structures manifests itself mainly in two effects. First, upon the embedding of oxygen ions and atoms in the titanium-dioxide film, oxygen vacancies, which serve as donor centers, are "healed"; therefore, the conductivity of TiO_2 lowers. Second, oxygen-plasma treatment of the TiO_2 film leads to the occurrence of a SiO_2 layer at the TiO_2–Si interface [2, 16]. The SiO_2 layer thicknesses (d_{SiO_2}) in the structures annealed at 500 and 750°C are 5.2 and 4.1 nm, respectively [2]. The smaller SiO_2 thickness in the samples annealed at 750°C is attributed to the closer packing of atoms in crystals of rutile, which exceeds anatase in stability, density, microhardness, refractive index, and permittivity. The TiO_2-film density is 3.84–3.9 g/cm^3 in the anatase phase and 4.25–4.26 g/cm^3 in the rutile phase [17].

Both above-mentioned effects determine the I–V characteristics of the structures. This conclusion is based on a decrease in the reverse current I_{rev} by almost three orders of magnitude and an increase in the rectification factor (see the table). As a result of sharp growth in the resistivity of the TiO_2 films after exposure to the oxygen plasma, a major part of the voltage $|U|$ drops at the titanium oxide and a significantly smaller part, at silicon. This fact explains the absence of photocurrent at $|U| < 2$ V. As the $|U|$ value is increased, the voltage drop at Si becomes larger, the space-charge region (SCR) increases, and the photocurrent grows.

To analyze the current flow through the investigated structures, we presented the "dark" I–V characteristics on the double logarithmic scale. At small positive gate potentials, the I–V characteristics of the samples annealed at 500°C are presented by straight-line segments with the slope $\tan\alpha = 1$ to the voltage axis; with an increase in voltage, $\tan\alpha$ increases from 1.5 to 2.0 (Fig. 8a, curves *1* and *3*). The reverse I–V characteristics in the range $0 \le |U| \le 10$ V are described by the linear voltage dependence of the current (Fig. 8a, curves *2* and *4*).

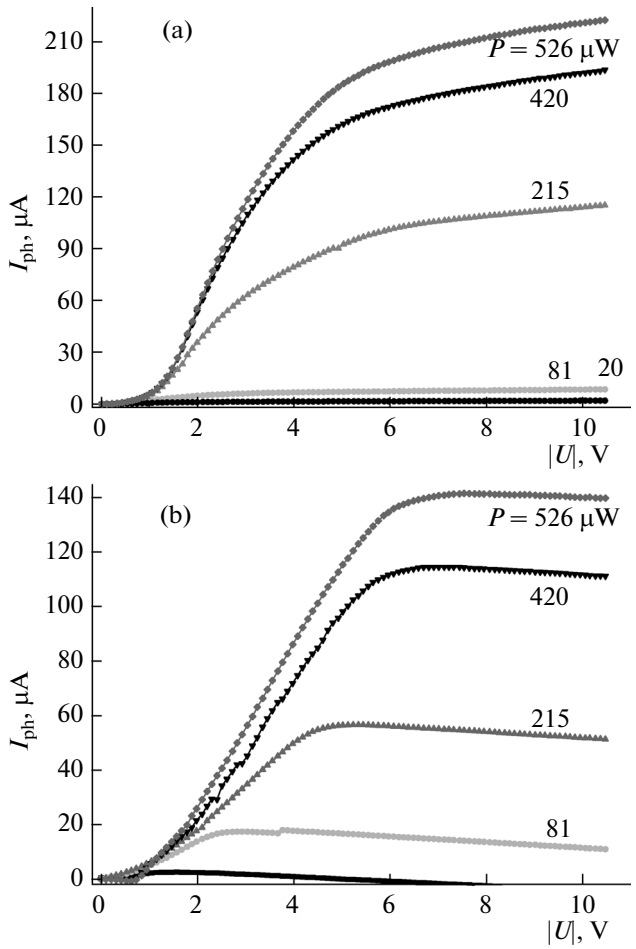

Fig. 6. Voltage dependence of the photocurrent for the samples annealed in argon at 750°C (a) not exposed and (b) exposed to the oxygen plasma.

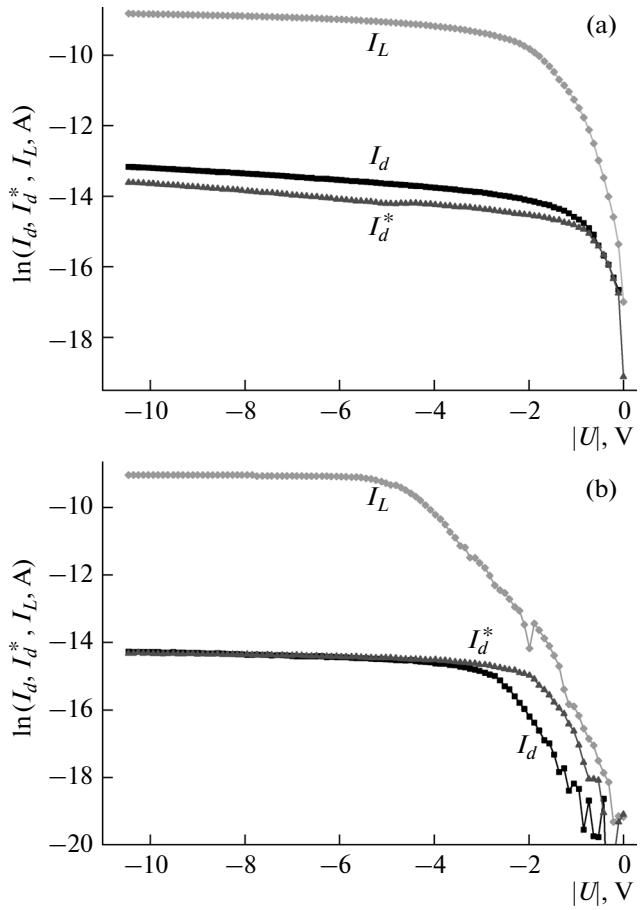

Fig. 7. Reverse I–V characteristics for the samples annealed in argon at 750°C (a) with and (b) without preliminary oxygen-plasma treatment. I_L is the current under illumination at $P = 526$ μW and I_d and I_d^* are the "dark" current before and after illumination, respectively.

The I–V characteristics of the structures annealed at 750°C without treatment in oxygen plasma are presented on the double logarithmic scale by straight-line segments with $\tan\alpha = 1.2$–2.6 (Fig. 8b, curves *1* and *3*).

Exposure to oxygen plasma leads to a decrease in the currents at positive and negative gate potentials, but the shape of the I–V characteristic remains almost unchanged. A decrease in the forward and reverse currents after oxygen-plasma exposure is attributed to the occurrence of a SiO_2 layer and a reduction in the conductivity of the titanium-oxide films.

The reported experimental data allow us to suggest that the "dark" I–V characteristics are determined by space-charge-limited currents in the TiO_2 film. This effect is especially pronounced in structures with the TiO_2 film in the anatase phase (Fig. 8a). At positive biases, the initial portions of the I–V characteristics are determined by the electron transport in the conduction band. As the voltage is increased, the I–V characteristics demonstrate portions of the power-voltage dependence of the current $I_{for} \propto |U|^n$ with $n = 2$ (Fig. 8a, curve *1*) and $n = 1.5$ (Fig. 8a, curve *3*), which are caused by the capture of electrons at trap centers. The results obtained are insufficient to characterize the energy distribution of the traps.

Without illumination, the reverse I–V characteristics demonstrate only the linear voltage dependence of the current. At negative gate biases, the voltage is distributed between the TiO_2 film and the SCR in silicon and the voltage drop at titanium oxide is insufficient to observe the effect of charge captured at traps on the I–V characteristics.

The photoelectric characteristics of TiO_2–Si structures are mainly determined by the absorption of light with a wavelength of $\lambda = 400$ nm in silicon and by the excitation of electrons from deep-level centers in titanium oxide. The lack of reverse current and photovoltage at positive gate biases under illumination is attributed to the extremely low potential-barrier heights at the TiO_2–Si interface. The latter is related to the similar electron affinities of titanium oxide (χ_{TiO_2} =

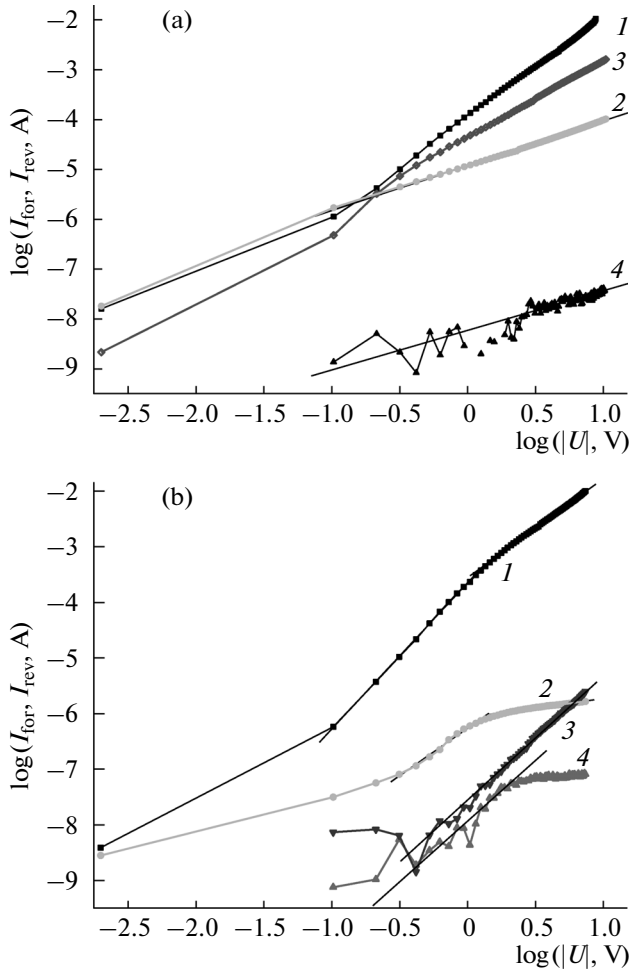

Fig. 8. "Dark" *I–V* characteristics for the samples annealed in argon at (a) 500°C and (b) 750°C. (*1*, *3*) Forward and (*2*, *4*) reverse *I–V* characteristics; (*1*, *2*) with and (*3*, *4*) without oxygen-plasma pretreatment.

4.5 eV) and silicon (χ_{Si} = 4.05 eV) with regard to the Fermi level F in n-Si with $N_d = 3 \times 10^{15}$ cm^{-3} relative to the bottom of the conduction band E_c ($E_c - F = 0.25$ eV).

The incident-light quantum energy is $h\nu = 3.1$ eV, whereas the band gap of titanium oxide in the anatase phase is $E_g = (3.2 \pm 0.1)$ eV. Therefore, in TiO_2 the light with λ = 400 nm can excite electrons mainly from deep centers. At negative gate potentials $|U| > 2$ V, the SCR in silicon becomes rather wide, electron–hole pairs are generated in it, and the photocurrent starts growing with increasing voltage (Fig. 3).

Under the effect of an external electric field, electrons penetrate deep into the semiconductor while holes are captured at surface states at the SiO_2–Si and SiO_2–TiO_2 interfaces. The transition of holes from the silicon valence band in TiO_2 is complicated by a high barrier [18]. After removal of the negative potential, the bending in Si sharply decreases and electrons diffuse to the SiO_2–Si interface due to the concentration gradient. Some of them pass to surface states and others diffuse into TiO_2 and are captured at deep traps. If a negative potential is applied to the gate again, then at rather high electric fields, electrons are thrown from deep centers to the TiO_2 conduction band, which leads to enhanced reverse currents. During sample storage, electrons captured at deep traps recombine with holes in the valence band and the excess "dark" conductivity decreases.

In samples of the second series annealed at 750°C, the incident light-quantum energy $h\nu = 3.1$ eV is comparable with the band gap of titanium oxide in the rutile phase E_g = 3.0 eV. This means that the bipolar generation of electron–hole pairs occurs in structures with the rutile film along with the generation of electrons from deep-level centers. The conductivity of the titanium-oxide films increases and the voltage drop at the SCR in silicon becomes larger. As a result, the generation of electron–hole pairs in the SCR of silicon starts at lower voltages than in the case of annealing at 500°C. In contrast to study [1], the photocurrent in the structures with the film of titanium oxide in the rutile phase was always higher than in samples of the first series.

The low photocurrents in the TiO_2–Si structures are attributed to the insufficient transparency of the titanium-dioxide films. As was shown by Gerasimenko et al. [19], after annealing of the TiO_2 films in an oxygen atmosphere at 450°C for 7.5 h the absorption coefficient at a wavelength of 400 nm is no larger than 20% and increases by 50% as the annealing temperature is elevated to 750°C (2 h).

The phenomenon of the residual reverse current after switching off the illumination is referred to as frozen photoconductivity. The current drop in time t at a fixed reverse voltage is described by the equation

$$I(t) = A\exp\left(-\frac{t}{\tau}\right) + B,$$

where A and B are some constants and τ is the decay constant. According to Fig. 5, the relaxation time is $\tau = (23 \pm 2)$ min, independent of the voltage in the range $U \geq 2$ V.

As was mentioned above, in the samples annealed at 750°C, the threshold voltage U_t corresponding to the occurrence of photocurrent decreases by a factor of two as compared with the structures annealed at 500°C. This effect is related to the higher conductivity of TiO_2 in the rutile phase and the smaller voltage drop at the insulator. Thus, the photocurrent arises at lower reverse voltages applied to the sample.

4. CONCLUSIONS

We carried out a set of experiments to study the electrical and photoelectric properties of V/Ni– TiO_2–Si–V/Ni structures in more detail. The

experiments allowed us to draw the following conclusions:

(i) we established correlations between the dc electrical and photoelectric properties of metal–TiO_2–Si structures and the structure and phase compositions of the TiO_2 films;

(ii) we demonstrated that, independent of the annealing temperature, oxygen plasma treatment leads to growth in the SiO_2 film at the semiconductor–insulator interface. The SiO_2 film favors a decrease in reverse currents. Under the same plasma treatment conditions, the silicon-oxide thickness in the TiO_2–Si structures with the TiO_2 film in the anatase phase is larger than in the case of the TiO_2 film in the rutile phase, which is explained by the lower density of anatase;

(iii) it was assumed that the conductivity mechanism in the V/Ni–TiO_2–Si–V/Ni structures is determined by space-charge-limited currents in the insulator film with traps;

(iv) on the V/Ni–TiO_2–Si–V/Ni structures, photocurrent is caused by the generation of electron–hole pairs in silicon; the lack of photocurrent at voltages of up to 2 V is related to the low transparency of the TiO_2 films to the incident light and weak absorption in the titanium-oxide film; and

(v) the structures fabricated using the described technology exhibit frozen photoconductivity after annealing at 500°C and preliminary treatment in oxygen plasma.

ACKNOWLEDGMENTS

This study was supported by the Ministry of Education and Science of the Russian Federation project no. 3.1206.2014/K.

REFERENCES

1. A. Janotti, C. Franchini, J. B. Varley, G. Kreesse, and C. G. van de Walle, Phys. Status Solidi RRL **7**, 199 (2013).
2. A. I. Kuznetsov, O. Kameneva, A. Alexandrov, N. Bityurin, Ph. Marteau, K. Chhor, C. Sanchez, and A. Kanaev, Phys. Rev. E **71**, 021403 (2005).
3. L.-B. Xiong, J.-L. Li, B. Yang, and Y. Yu, J. Nanomater. **2012**, 831524 (2012).
4. A. I. Kuznetsov, O. Kameneva, A. Alexandrov, N. Bityurin, K. Chhor, and A. Kanaev, J. Phys. Chem. B **110**, 435 (2006).
5. A. Sirisuk, E. Klansorn, and P. Praserthdam, Catal. Commun. **9**, 1810 (2008).
6. N. Sakai, R. Wang, A. Fujishima, T. Watanabe, and K. Hashimoto, Langmuir **14**, 5918 (1998).
7. N. Sakai, A. Fujishima, T. Watanabe, and K. Hashimoto, J. Phys. Chem. B **105**, 3023 (2001).
8. N. Sakai, A. Fujishima, T. Watanabe, and K. Hashimoto, J. Phys. Chem. B **107**, 1028 (2003).
9. N. Bityurin, A. I. Kuznetsov, and A. Kanaev, Appl. Surf. Sci. **248**, 86 (2005).
10. J. Huang, M. Wang, J. Zhao, N. Gao, and Y. Li, Appl. Rad. Isotopes **54**, 475 (2001).
11. E. Yagi, R. R. Hasiguti, and M. Aono, Phys. Rev. B **54**, 7945 (1996).
12. V. M. Kalygina, V. A. Novikov, Yu. S. Petrova, O. P. Tolbanov, E. V. Chernikov, S. Yu. Tsupii, and T. M. Yaskevich, Semiconductors **48**, 961 (2014).
13. M. Chra Sekhar, P. Kondaiah, S. V. Jagadeesh Chandra, et al., Surf. Interface Anal. **44**, 1299 (2012).
14. K. Shubham and R. U. Khan, J. Nano Electron. Phys. **5**, 01021 (2013).
15. P. Kondaiah, M. Chandra Sekhar, S. V. Jagadeesh Chandra, R. Martins, S. Uthanna, and E. Elangovan, IOP Conf. Ser.: Mater. Sci. Eng. **30**, 012005 (2012).
16. B. S. Richards, J. E. Cotter, C. B. Honsberg, et al., in *Proceedings of the 28th IEEE Photovoltaic Specialists Conference PVSC* (Anchorage, 2000), p. 5.
17. S. Springer, Diploma Work in Physics (Inst. Phys. Matiere Complexe, Lausanne, EPFL, 2004).
18. Yu. S. Milovanov, I. V. Gavrilchenko, V. Ya. Gayvoronsky, A. I. Kuznetsov, and V. A. Skryshevsky, Ukr. J. Phys. **57**, 545 (2012).
19. Yu. V. Gerasimenko, V. A. Logacheva, and A. M. Khoviv, Kondens. Sredy Mezhfaz. Granitsy **12**, 113 (2010).

Translated by E. Bondareva